Analysing texture features from individual observer simulations

Yuan Tian, Fereshteh Mirjalili and Jean-Baptiste Thomas

Department of Computer Science, Norwegian University of Science and Technology, Gjøvik, Norway
Emails: yt6580@rit.edu; fereshteh.mirjali@ntnu.no; jean.b.thomas@ntnu.no

We investigated the impact of simulated individual observer colour matching functions (CMFs) on computational texture features. We hypothesised that most humans perceive texture in a similar manner, hence a texture indicator that is the least dependent on individual physiology of human vision would be most likely a potential fit to serve as quantified visually perceived texture. To this end, the following strategy was implemented: hyper-spectral image textures were converted into XYZ images for individual observer CMFs, contrast sensitivity function (CSF) filtering was subsequently applied on the XYZ images for visual simulation. Two types of texture features were extracted from the filtered images. Finally, the difference between the texture features were analysed for observers with disparity in their CMFs.

Introduction

Texture perception, measurement and modelling has been largely investigated, yet we do not fully understand the mechanism by which humans perceive texture [1-3]. Several texture indicators have been developed to quantify texture [4], and the relation between those indicators and human judgement is a current topic of research [5-6]. In this study, we investigate the impact of individual observer colour matching functions (CMFs) on two types of texture features. The motivation behind this work is based on the following hypothesis: if humans can communicate about appearance, this implies that despite individual differences, humans have a similar cognitive way of interpreting and representing material appearance. With texture being one of the main appearance attributes [7], it means that texture features which are consistent across changes of vision model's parameters, are more likely to be good quantified representatives of visual perception of texture. If this hypothesis could be verified, we could simply use simulated observer CMFs to compare various texture features in terms of their performance in quantifying visual texture, assuming that we have access to an appropriate vision model. To test our hypothesis, we used two classes of texture features in this study. The vision model employed is based on individual CMFs and a Contrast Masking method. A series of image textures were selected from the HyTexiLa [8] texture dataset. After filtering the images with contrast sensitivity functions (CSFs), the texture features of the images were computed. Finally, the texture features corresponding to two groups of individual observers were compared to find out whether any of the features has relatively similar values for the two observer groups. Figure 1 illustrates the methodology implemented in this study to test our hypothesis.
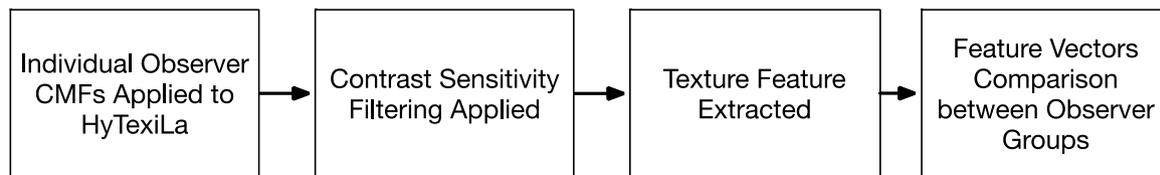
Figure 1: The implemented methodology to verify our hypothesis: if humans can communicate about appearance, this implies that despite individual differences, humans have a similar cognitive way of interpreting and representing material appearance, including visual texture.

Experiment

A vision model for individual colorimetric observers

In this study, we used the individual observer colour matching functions modelled by Asano [9]. The creation of the model involved three steps: colour matching experiments, estimating physiological parameters by the aid of an optimisation process using the individual observer colorimetric model, and computing the individual observer colour matching functions. In the colour matching experiments, the colour stimuli were four LED primaries, and 151 colour-normal observers were participated in the experiments. For each subject, five colour matches were used, and each matching was repeated three times. The observers' ages ranged from 20 to 69 years old, and their inter-variability was tested using the Mean Colour Difference from the Mean (MCDM) parameter. The colour matching data were used in the individual observer colorimetric model, shown in Equation 1.

$$lms-CMFs = f\left(a,\ v,\ d_{lens},\ d_{macula},\ d_L,\ d_M,\ s_L,\ s_M,\ s_S\right) \tag{1}$$

where a is an age of an observer, v is a visual angle in degree, d_{lens} is % deviation from an average for lens pigment density, d_{macula} is % deviation from an average for peak optical density of macular pigment, d_L, d_M, and d_S are % deviations from averages for peak optical densities of L-, M-, and S-cone photopigments, respectively, s_L, s_M, and s_S are deviations in nm from averages for λ_{max} shifts of L-, M-, and S-cone photopigments, respectively. The model output was lms-CMFs which is also known as cone fundamentals [9]. Each Individual lms-CMF was converted into the corresponding xyz-CMF by a linear transform obtained from a linear regression between the CIE 1964 standard colorimetric observer and the average lms-CMFs. The resulting CMFs are depicted in Figure 3.

Image texture selection

The HyTexiLa dataset [8], including five classes of hyperspectral images namely textile, wood, stone, food, and vegetation were employed as image textures in this study. Five hyperspectral images were chosen from the textile class, and two images were chosen from each of the other four classes. The images were chosen in a way that they would represent a variety of texture patterns and possibly texture features. Figure 2 shows the sRGB representations of the selected images. The hyperspectral data of the images include the spectral reflectance of each image pixel, within the wavelength range of 405.37 to 780 nm with a 3.19 nm interval.
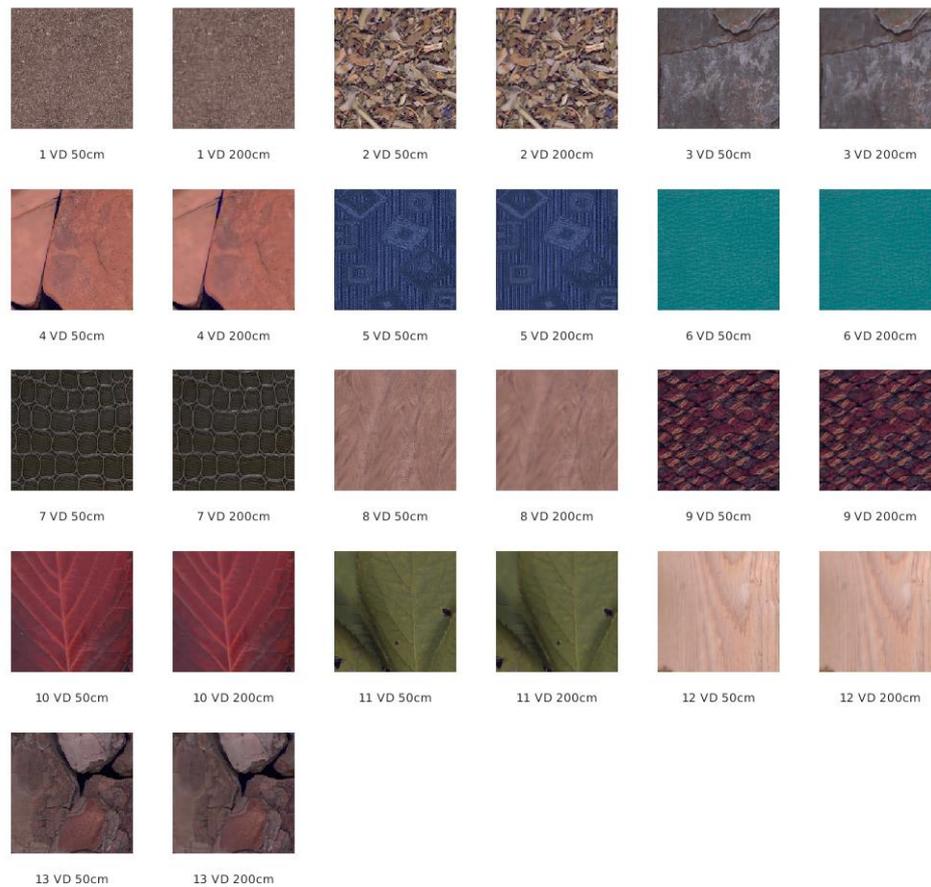
Figure 2: sRGB renderings of the 13 selected HyTexiLa images after applying CSF at the viewing distances of 50 cm and 200 cm.

Contrast sensitivity function filtering

Before applying the colour sensitivity filter, CSF, a colour space transformation was required from XYZ into YCbCr. The conversion followed the method by Pedersen and Farup [10]. The authors convert the sRGB images to the corresponding YCbCr representations using the following routine: sRGB → XYZ → RGB → YCbCr → sRGB by defining a specific set of primaries. In this study, the hyperspectral images were first converted to the corresponding XYZ images and then the Pederson and Farup's routine was used to convert the XYZ to the corresponding YCbCr images. To reduce the computational time, all images were downsampled from the original size of 1024×1024 pixels to 205×205 pixels.

The YCbCr images were subsequently decomposed into a set of low pass bands and several sets of high pass bands using the Shearlets tool [11]. The high pass bands were filtered by the colour sensitivity function, CSF, from Barten [12], with separate luminance Y channel, and chrominance Cb and Cr channels. The filtering method by Nadenau [13] was used for considering local activity in the intra channel masking. For applying the CSF, two viewing distances, i.e. 50 cm as the typical reading distance, and 200 cm as the long observation distance were used. Moreover, the luminance of the screen and the surround as the input variables to the CSF were set to 80 cd/m² and 20 cd/m², respectively. In total, 3926 images for 13 image textures × 151 observers of CMFs × 2 viewing distances for colour sensitivity filtering were used in this study.

Texture features

After CSF filtering, the YCbCr images were used to compute first-order and second-order statistic texture features, separately for the luminance Y and chrominance Cb and Cr channels of the image textures. The first-order image statistics are the simplest features for characterising textures, and refer to the statistical parameters such as mean, standard deviation, and central moments. They are computed either directly from the image pixel values, or from the image histogram. In this study, the mean and the standard deviation of pixel values were computed for the luminance Y channel and the chrominance Cb and Cr channels of the images as the first-order texture features.

While first-order statistics provide information about the distribution of the image pixel values, they do not provide any information about the relative positions of such pixels within the image. Examining the relationship between pair of pixels across the image can be conducted through the second-order statistical features. One of the most well-known second-order statistics for texture analysis is the Co-occurrence Matrix (CoM).

A grey level co-occurrence matrix (GLCM) is a two-dimensional matrix comprising the probability of occurrence of two pixels with specific pixel values at a particular displacement of distance and rotation angle [14]. A number of statistics can be derived from the GLCM. Haralick *et al.* [14] proposed fourteen different features. However, it has been demonstrated that some of these features are highly correlated and only five of them including energy, contrast, correlation, entropy, and homogeneity could be sufficient for texture analysis purposes [15]. These five features were computed for the luminance Y channel of the image textures in this research.

Before extracting the texture features, the output YCbCr images from the colour sensitivity filtering were linearly tone-mapped for each pixel value to be within the range of 0-255. For GLCM features, the pixel values were rounded into integers, before building the GLCM matrix. For each YCbCr image, the GLCM feature vector had the size of [1×5], comprising the energy, contrast, correlation, homogeneity, and the entropy of the luminance Y channel, while the first-order mean-std feature vector had the size of [1×6], comprising the mean and the standard deviation of the luminance Y and chrominance Cb and Cr channels.

Results and discussion

Figure 3 (left) shows the xyz colour matching functions of the 151 individual colorimetric observers used in this study [9]. It can be seen in Figure 3 that the CMFs of these observers are distributed around the average CMF of all observers (the black curves in Figure 3 (left)) for x, y, and z CMFs. It clearly illustrates that despite being similar in trend, individual observers have different CMFs. For each observer, the root mean square error (RMSE) of their CMF from the average CMF were determined. The histogram of such RMSE values are depicted in Figure 3 (right).

To verify our hypothesis, we required two distinct groups of individual observers with meaningful disparity between their respective CMFs. The observers with RMSEs smaller than the 50th percentile of the RMSE distribution were taken as the "average observer" group. The second group contained all observers including the observers in the "average observer" group. We expected that these two groups of observers would have meaningful differences in their colour vision, given the difference in their average CMFs. Principal component analysis (PCA) was conducted on x, y, and z colour matching data of the 151 observers in order to better visualise the dispersion of the observers in a two-dimensional space. The first two principle components correspond to 95%, 94% and 99% of data variance for x, y, and z colour matching data, respectively. Figure 4 illustrates the dispersion of the 151 individual

observers in the corresponding principle component spaces. Blue and red markers in Figure 4 belong to the observers in the "average observer" group, and the "dispersed observers" group, respectively. All the markers form the "all observer" group.
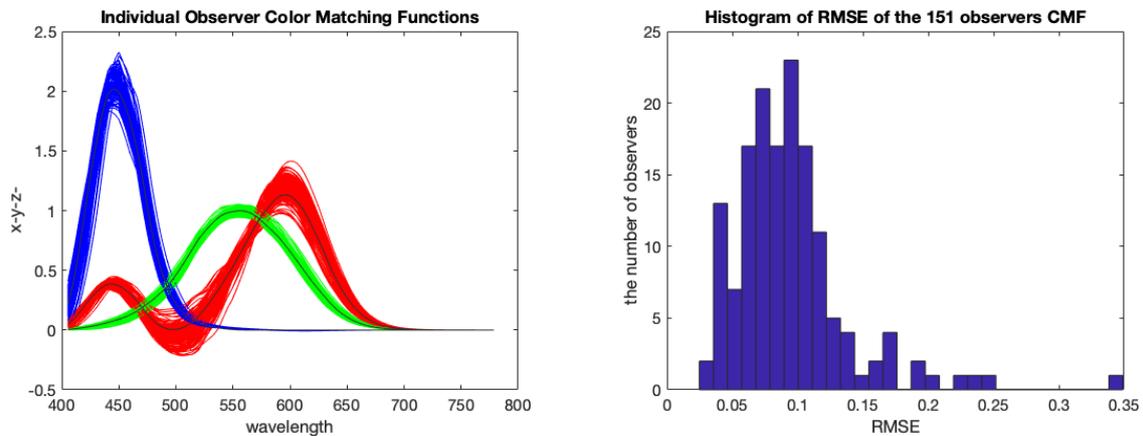

Figure 3: (Left) x, y, and z CMFs of the 151 individual observers used in our experiment. The black line is the average CMFs. (Right) the histogram of RMSE of the 151 observers' CMFs compared to the corresponding average CMFs. This histogram provides a visualisation of the dispersion of the individual observers' CMFs. Note that no CMF is exactly at the average position.
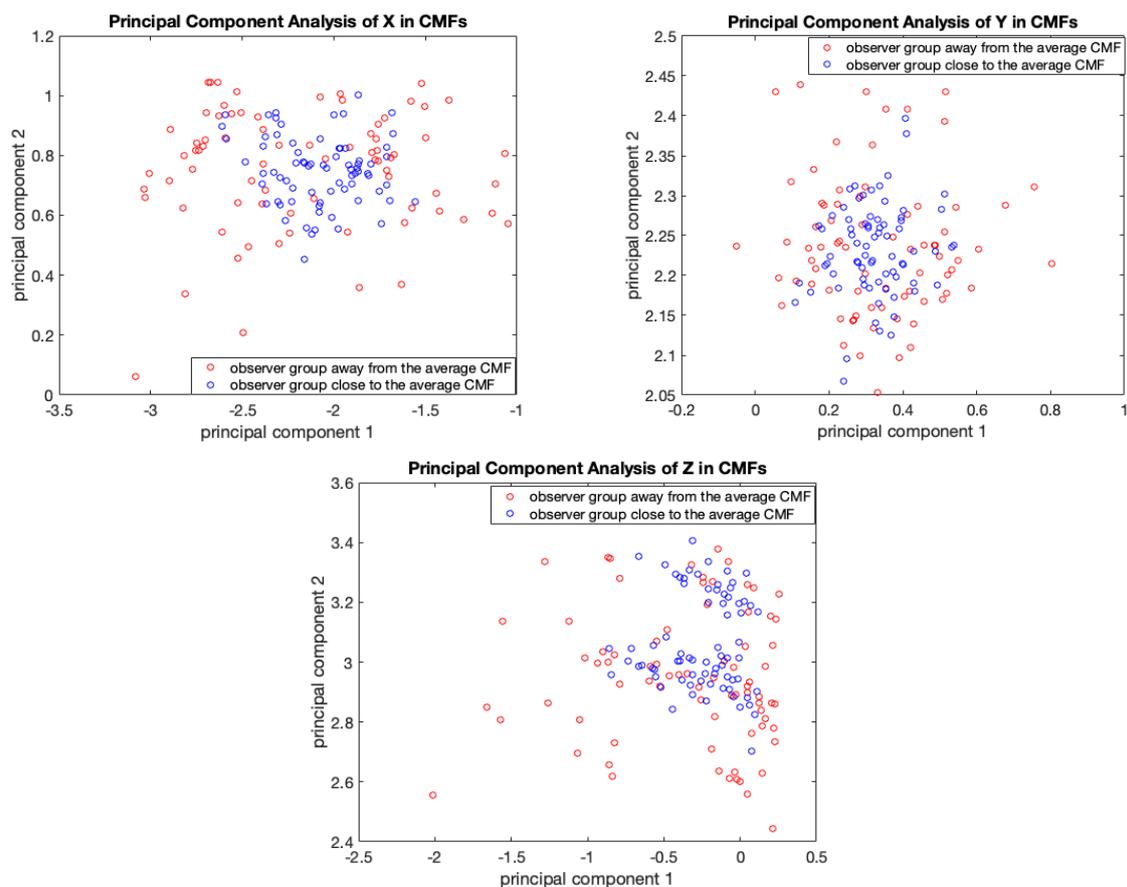

Figure 4: Distribution of the 151 individual observers in the corresponding principle component spaces. Blue and red markers in Figure 5 belong to the observers in the "average observer" group, and the "dispersed observer" group, respectively. They together form the "all observer" group.

To compare the texture features between the two observer groups, the three-dimensional volume constituted by the texture feature vectors was calculated for each group and each set of texture feature vectors i.e. GLCM and mean-std feature vectors, using the *convhull* function in MATLAB [16]. The volume ratio of the two groups was subsequently calculated using Equation 2:

$$Volume\ ratio = 10\,log_{10}(\frac{V_T}{V_A}) \tag{2}$$

where V_T is the volume constituted by the texture feature vectors of the "all observers" group, and V_A is the volume constituted by the texture feature vectors of the "average observer" group.

Figure 5 shows the volume ratios corresponding to the two texture features i.e. GLCM features and mean-std features, calculated for the 13 YCbCr images after CSF filtering for the viewing distances of 50 cm and 200 cm. The volume ratio around 0 shows that there is no difference between two observer groups in texture features, while the volume ratio greater than 10 represents there is at least 1 order of magnitude difference in volumes of texture feature vectors between two observer groups. In the graph of volume ratio of GLCM features, 7 out of 13 images have the volume ratios greater than 10. And 6 out of that 7 images have lower volume ratios down to less than 10, with the higher viewing distances. That could be explained by GLCM takes into account only luminance channel where the most textures information of the image is preserved. With higher viewing distance, textures are blurred and the disparity of individual observers in higher spatial frequency information also decreases. Because the texture perception depends on the intensity gradient perception. For images 1, 8 and 12 in viewing distance of 200 cm, the values of the volume ratio are -13.80, -14.16 and -13.50. They are not showing in the graph because they are negative, meaning that the volumes of the average observer groups are bigger. That indicates that the feature vectors between two observer groups are similar enough so that the noise through the computation makes the results fluctuated. Images 1, 6, 9, 11 and 13 shows similar GLCM feature between two observer groups in both viewing distances. If combining the assumption that GLCM features represent human observer texture feature perception and the assumption of individual observers tend to have similar texture perception although various with colour matching functions, the results of the GLCM graph can infer that the similar texture perception trend depends on the images and viewing distances.
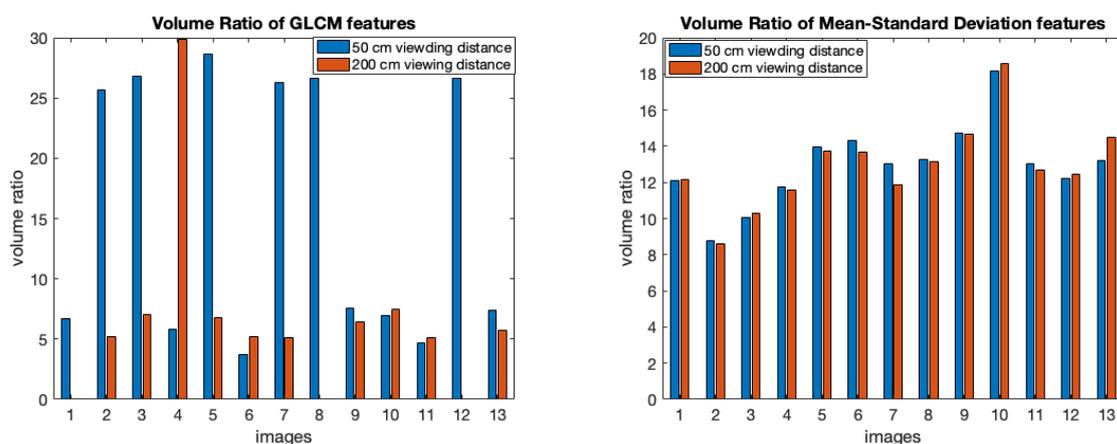

Figure 5: Volume ratios corresponding to the two texture features i.e. GLCM features and mean-std features, calculated for the 13 YCbCr images after CSF filtering for the viewing distances of 50 cm and 200 cm.

In the graph of volume ratio of Mean-Standard Deviation feature, most of images have the volume ratio around 10 while images 2 and 3 have the volume ratio below 10. That different from in GLCM features could be because the Mean-Standard Deviation takes chromatic channels into account beside the luminance channel, which causes that the variance of individual observer CMFs has more influence on Mean-Standard Deviation features. The one order of magnitude difference in texture feature volumes appear to be small compared to their original orders of magnitude. But the definition of the similar texture features needs to be further explored. However, there are no obvious difference in volume ratio when increasing the viewing distance. The reason is that the contrast sensitivity function filtering with different viewing distances does not change the intensity distribution of the images.

Conclusions

This study explores a methodology to investigate the impact of individual observer colour matching functions on simulated texture features. With the hypothesis that individual observers with various colour matching functions tend to have similar perceived textures, the results by the two simulated features can be explained in the view of our hypothesis, however this is preliminary and requires further test and analysis to develop strong observations. If it is found that texture perception is generally similar, but that the similarity depends on viewing distances and images, the GLCM features might become one of representatives of the perceived texture features. Mean-Standard Deviation features include limited indicators of texture features compared to GLCM, but the results are explained from the hypothesis with some variations.

Future work includes the verification of the hypothesis. A first step toward that should be based on visual experimentation based on numbers of observers. It is important to develop also the test of several texture features on huge databases.

References

1. Julesz B (1975), Experiments in the visual perception of texture, *Scientific American*, **232** (4), 34-43.

2. Tamura H, Mori S and Yamawaki T (1978), Textural features corresponding to visual perception, *IEEE Transactions on System, Mann and Cybernetics*, **8** (6), 460-473.

3. Gibson JJ and Bridgeman B (1987), The visual perception of surface texture in photographs, *Psychological Research*, **49** (1), 1-5.

4. Xie X and Mirmehdi A (2008), A galaxy of texture features, *Handbook of Texture Analysis*, Mirmehdi M, Xie X and Suri J (eds.), 375-406, Imperial College Press.

5. Benco M, Hudec R, Kamencay P, Zachariasova M and Matuskal S (2014), An advanced approach to extraction of colour texture features based on GLCM, *International Journal of Advanced Robotic Systems*, 11 (7), 104:1-8.

6. Mirjalili F and Hardeberg JY (2019), Appearance perception of textiles: a tactile and visual texture study, *Proceedings of the 27th Color Imaging Conference*, 43-48, Paris (France).

7. CIE (2006), A framework for the measurement of visual appearance, *CIE 175:2006 Report*, Central Bureau of the International Commission on Illumination (CIE), Paris (France).

8. Khan HA, Mihoubi S, Mathon B, Thomas J-B and Hardeberg JY (2018), HyTexiLa: High resolution visible and near infrared hyperspectral texture images, *Sensors*, **18** (7), 1-30.

9. Asano Y (2015), Individual colorimetric observers for personalized color imaging, *PhD Thesis*, Rochester Institute of Technology (USA).

10. Pedersen M and Farup I (2012), Simulation of image detail visibility using contrast sensitivity functions and wavelets, *Proceedings of the 20th Color and Imaging Conference*, 70-75, Los Angeles (USA).

11. Kutyniok G, Lim W-Q and Reisenhofer R (2016), ShearLab 3D: Faithful digital shearlet transforms based on compactly supported shearlets, *ACM Transactions on Mathematical Software*, **42** (1), 5:1-42.

12. Barten PGJ (2003), Formula for the contrast sensitivity of the human eye, *Image Quality and System Performance*, **5294**, 231-238.

13. Nadenau M (2000), Integration of human color vision models into high quality image compression, *PhD Thesis*, Ecole Polytechnique Federale de Lausanne (Switzerland).

14. Haralick RM, Shanmugam K and Dinstein I (1973), Textural features for image classification, *IEEE Transactions on Systems, Man, and Cybernetics*, **3** (6), 610-621.

15. Palm C (2004), Color texture classification by integrative co-occurrence matrices, *Pattern Recognition*, **37** (5), 965-976.

16. MATLAB R2019a (2019), *Image Processing and Computer Vision Toolbox*, The MathWorks, Inc.